AUTOMATIC OPTIC DISK DETECTION FROM LOW CONTRAST RETINAL IMAGES OF ROP INFANT USING MATHEMATICAL MORPHOLOGY

Viranee Thongnuch[1], Bunyarit Uyyanonvara[2]
[1, 2]School of Information & Computer Technology
Sirindhorn International Institute of Technology, Thammasat University,
131 Moo 5, Tiwanont Road, Bangkadi, A. Maung, Pathum Thani 12000,Thailand

Abstract— **Retinopathy of Prematurity (ROP) is a developmental disease used to describe abnormal blood vessels and scar tissue growing inside and over the retina of the eye. Early symptom detection can prevent childhood blindness. Automated screening would be required, however general-method edge detection algorithms often fail to detect the optic disk due to fuzzy boundaries, inconsistent image contrast or missing edge features because , especially in case of infant, image acquisition process has to be very quick and in low light condition. This paper presents an algorithm for segmentation of optic disk boundary in low-contrast images. Histogram equalization and average filtering techniques were used to enhance Red band of the original low-contrast retinal image. The blood vessel was eliminated from the retinal image using the morphology closing. Optic disk localization is then achieved using optimized mathematical morphology and connected labeling. The result of 30 infant's retinal images with ROP condition were validated with experts' hand-drawn ground truth. The result is quite successful with the accuracy of 87.0 % for retinal images in ROP Infant.**

Keywords— **Optic Disk, Retinopathy of Prematurity, Diabetic retinopathy, Mathematical morphology, Morphology closing**

I. INTRODUCTION

Retinopathy of Prematurity (ROP) is a developmental disease used to describe abnormal blood vessels and scar tissue growing inside and over the retina of the eye. The incidence of ROP rises with lower gestational age and birth weight. In patients with ROP, the premature baby's blood vessels in the eye are very sensitive to oxygen and light which makes the blood vessels stop growing and new abnormal blood vessels grow instead of normal retinal blood vessels. It usually affects babies and leads to blindness or poor vision. Precise localization of optic disk boundary is an important sub problem of higher level problems in ophthalmic image processing. Specifically, in proliferative diabetic retinopathy, fragile vessels develop in the retina, largely in the OD region, in response to circulation problems created during earlier stages of the disease. If the optic disk has been identified, the position of areas of clinical importance such as the fovea may be determined. Moreover, OD detection is fundamental for establishing a frame of reference within the retinal image and is, thus, important for any image analysis application.

Many techniques have been purposed including detection of the OD regions by clustering the brightest pixels in retinal image and locating potential OD area. One of them is based on a model of vascular structure by Foracchia et al.[1]. The authors used a geometrical parametric model locating at the center point of OD. Akita et al.[2], traced the parent-child relationship between blood vessels segments, tracking back to the center of the optic disk. This also proposed robust detection of the blood vessels, which is difficult in images of diseased retina where even quite sophisticated algorithms detect false positives along the edges of white lesions and along the optic disk. Lalonde et al.[3] used pyramidal decomposition and Hausdorff-based template matching that is guided by scale tracking of large objects using multi-resolution image decomposition. This method is effective, but rather complex. In three dimensional reconstructions of conventional stereo optic disk image procedures, Kong et al.[4] presented the resulting 3 dimensional contour images that show optic disk structure clearly and intuitively, helping physicians in understanding the stereo disc photograph. Cox and Wood[5] presented a semi-automated method to indicate external points on the boundary which were automatically connected by tracing along the boundary. Morris and Cox[6] initially presented a completely automatic method which traced between points on the boundary identified automatically by their grey level gradient properties. Sinthanayothin et al.[7] used the rapid intensity variation between the dark vessels and the bright nerve fibers to locate the optic disk. However, they found that this algorithm often failed for fundus images with a large number of white lesions. Lee[8] also applied an active contour model to high resolution images centered on the optic nerve head and his problem caused by the boundary of the pallor and by very faint or missing edges. Li et al.[9][10] , used PCA and ASM technique to apply in detecting the optic disk centre and approximate the optic disk area by using "disk space" but this algorithm failed in unclear shape of optic disk. Kavitha[11] used morphological operations and multilevel thresholding to extract the brighter regions that includes optic disc and exudates. Jelinek et al.[12] used Canny edge detection, template matching and Haar transform to detect optic disk boundary. The most effective method has been reported by Osareh et al.[13], Mendels et al.[14], Chanwimaluang and Fan[15] based on the active-contour model or snake. However, most of techniques mentioned above have been mainly focused on adult retinal images where the retina is well developed. In this paper, we present the algorithm that is effectively detected optic disk from the infant's retinal images. The algorithm is based on mathematical morphology technique to extract the optic disk from the retinal image as described in the following sections.

II. METHODOLOGY

Step 1: Changing the retinal image into red channel.
In order to change the image into the red channels only because the color of optic disk always primitive in Red channel as shown in figure1(a).

Step 2: Using Histogram Enhancement
In the infant's retinal image, the image is often blurred. Most of the information is packed in the lower order parts of the image histogram. Improvements in the contrast can make this algorithm more efficient, but more importance it will help to perceive the images better. The transformation is done as a point processing since the enhancement of any pixel is dependent only on red channel at that point. Histogram equalization automatically determines a red channel transformation function that produces an output image with a uniform histogram and improves retinal image contrast as shown in figure1(b).

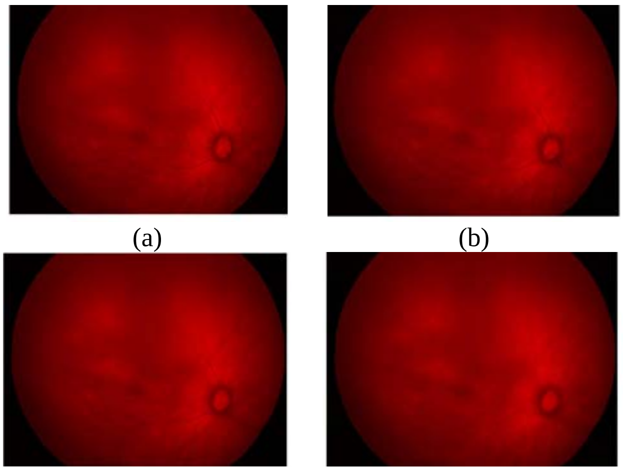

(a) (b) (c) (d)

Figure1. (a) The Optic disk in Red Channel (b) Histogram Equalization (c) Averaging filter for smoothing the image (d) Closing Image for removing blood vessel

Step 3: Using Average filter
Average filter is used to remove noise in the retinal image and make a picture smooth as shown in figure1(c).

Step 4: Using Morphological Closing
We try to use this property to remove vessel in the image. Morphological closing is based on two fundamental operation dilation and erosion which is defined by (1)

$$A \bullet B = (A \oplus B) \Theta B \qquad (1)$$

In the retinal image, that always consists of some spot and exceed pixels that caused by noise and blood vessels. These unwanted pixels are necessary to eliminated in order to receive the exact optic disk. The elimination of unwanted pixels uses Image Closing technique, which is morphological operation. Result of this step that has smoothes image without blood vessel as shown in figure 1(d).

Step 5: Using canny edge detection
The Canny edge detection applied to Red channel of RGB to find the edge of the optic disk. The result of this edge detector is a binary image in which the white pixels closely approximate the true edges of the original image as shown in figure2(a).

Step 6: Mask the edge of the object
Using convolution mask to add pixel into the boundary line, to give more detail in boundary line like the image in figure2(b).

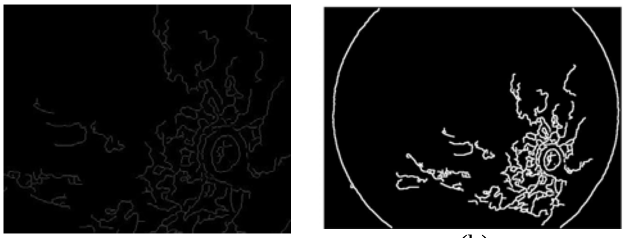

(a) (b)

Figure2. (a) Canny Edge detection (b) Canny edge detection after mask the edge line

Step 7: Using Dilation and filling the hole.
Dilation causes objects to dilate or grow in size by adding pixels to the boundaries of the object in an image. We processed the image the image using disk shaped structured element that defines the neighborhood region around its origin with a radius of 5 to connect the area within the image.
The dilation of A by B, denoted by $A \oplus B$, is defined as (2)

$$A \oplus B = \{x \mid (\hat{B})_x \cap A \neq \varnothing\} \qquad (2)$$

Dilation is achieved by assigning 1 to the origin of the structuring element when it overlaps, even partially, the object as shown in Figure3(a). Next we develop a simple algorithm for region filling based on set dilations, complementation, and intersections. The objective is to fill the entire region with 1's as shown in figure3(b).

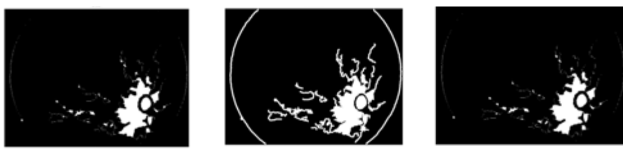

(a) (b) (c)

Figure3. (a)Dilate the image (b)Fill the hole within the image (c) Erode the image

Step 8: Using Erosion
The concept of erosion is to contract the boundary of an object in an image. Erosion is achieved by assigning 1 to the origin of the structuring element when it entirely

overlaps the object as shown in figure3(c). We use erosion to separate the optic disk object from other objects. The erosion of A by B, denoted by $A\Theta B$,is defined as(3)

$$A\Theta B = \{x \mid (B)_x \subseteq A\} \qquad (3)$$

Step 9: Using Connected Component Labeling
We label the area within the image by using 4-neighborhood connecting. All connected pixels with the same input value are assigned the same identification label. figure4(a) shows the connected component labeling in the algorithm.

Step 10: Remove noise from the image.
In order to remove a small part, we count each individual component in the binary image. If the number of pixels in a component are not in range between 1200 to 1600 pixels (round shape of optic disk), we will remove it. After that it will leave only optic disk within the image as show in figure4(b). In figure5(a-b), it presents the example of successful result in the different shape and size of optic disk.

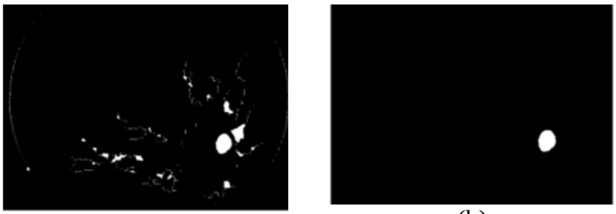

(a) (b)

Figure4. (a)Noise within the image (b) After noise removing

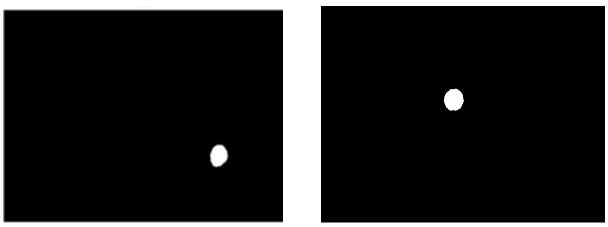

(a) (b)

Figure5. (a-b) The example of successful result

DIAGRAM I
THE DIAGRAM OF METHODOLOGY

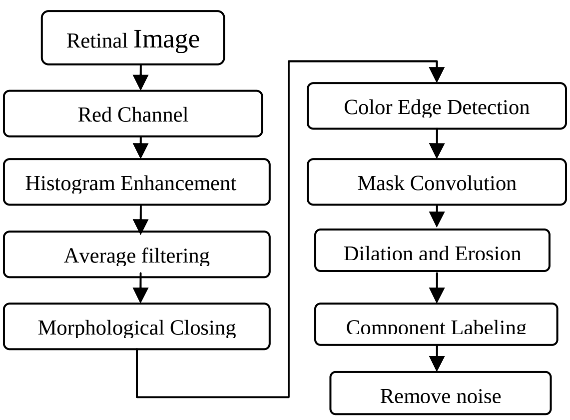

III. EXPERIMENT VERIFICATION

The results were clinically validated in this step. All images in our test set were sent to ophthalmologist to identify the OD manually. Expert ophthalmologist hand-labelled the optic disk on the screen. All optic disk pixels were set to white and all non-optic disk pixels set to black. The new image was saved as a ground-truth which will be used for comparison. All the OD's which are automatically detected by our system were then compared with clinician's hand-drawn ground truth. The result is evaluated quantitatively by comparing the resulting detection with ophthalmologists' hand-drawn ground-truth images pixel by pixel. Figure6 shows an example of both ground truth image and our detection result. The hand-drawn and detected optic disk images are represented in white.

(a) (b)

Figure6 (a) Clinician's hand-drawn ground truth (b) Detected pixels from mathematical morphology

Four values, namely TP, TN, FP and FN which stand for true positive, true negative, false positive and false negative, respectively[17] were used as measurements. True Positive (TP) is a number of optic disk pixels correctly detected, False Positive (FP) is a number of non-optic disk pixels which are detected wrongly as optic disk pixels, False Negative (FN) is a number of optic disk pixels that were not detected and True Negative (TN) is a number of non-optic disk pixels which were correctly identified as non-optic disk pixels as shown in table 1.

TABLE I
OPTIC DISK VERIFICATION

	OD Present	OD Absent
OD detected	True Positive(TP)	False Positive(FP)
OD not detected	False Negative(FN)	True Negative(TN)

In order to evaluate the performance of the algorithm quantitatively, the measure of accuracy, sensitivity and specificity are also defined (Eq. (4),(5) and Eq. (6))
The accuracy shows the performance of this method, sensitivity shows the proportion of optic disk pixels which positively detected and the specificity shows the proportion of non-op disk pixels which negatively detected.

$$Accuracy = \frac{(TP+TN)}{(TP+FN+TN+FP)} x100 \quad (4)$$

$$Sensitivity(\%) = \frac{TP}{TP+FN} x100 \quad (5)$$

$$Specificity(\%) = \frac{TN}{TN+FP} x100 \quad (6)$$

After all the thirty retinal images were processed, they were compared with the hand-drawn ground-truth images marked by ophthalmologist and the result will be discussed in the next section.

IV. EXPERIMENTAL RESULTS

Two set of images were used in this experiment. The first set of 30 images was images from ROP infants. The result of detection for the fist set is demonstrated in table 2.

TABLE II
THE EXAMPLES OF ACCURACY, SENSITIVITY AND SPECIFICITY RESULT IN RETINAL IMAGE WITH ROP CONDITION

Image	TP	TN	FP	FN	Ac(%)	Se(%)	Sp(%)
A11g	1262	0	246	14	82.9	98.9	0.0
A12g	1405	0	204	1	87.3	99.9	0.0
A13g	1344	0	202	27	85.4	98.0	0.0
A17g	1562	0	132	94	87.4	94.3	0.0
A19g	1627	0	192	44	87.3	97.4	0.0
A5g	1400	0	315	1	81.6	99.9	0.0
A6g	1595	0	115	29	91.7	98.2	0.0
A7g	1383	0	169	73	85.1	95.0	0.0
A8g	1461	0	168	17	88.8	98.8	0.0
A9g	1412	0	165	53	86.6	96.4	0.0
B3g	2107	0	291	124	83.5	94.4	0.0
C10g	1371	0	162	136	82.1	91.0	0.0
C11g	1266	0	156	4	88.8	99.7	0.0
C12g	1320	0	164	0	88.9	100.0	0.0
C13g	1398	0	116	69	88.3	95.3	0.0
C2g	1396	0	270	26	82.5	98.2	0.0
C6g	1417	0	181	52	85.9	96.5	0.0
C7g	1351	0	131	33	89.2	97.6	0.0
C8g	1328	0	142	9	89.8	99.3	0.0
C9g	1366	0	85	139	85.9	90.8	0.0
D10g	1685	0	159	45	89.2	97.4	0.0
D11g	1831	0	114	104	89.4	94.6	0.0
D14g	1799	0	56	82	92.9	95.6	0.0
D18g	1752	0	109	224	84.0	88.7	0.0
D19g	1773	0	82	190	86.7	90.3	0.0
D2g	1318	0	180	29	86.3	97.8	0.0
D4g	1421	0	161	82	85.4	94.5	0.0
D6g	1489	0	133	45	89.3	97.1	0.0
D7g	1402	0	139	46	88.3	96.8	0.0
D8g	1479	0	135	17	90.7	98.9	0.0
				Overall	**87.0**	**96.4**	**0.0**

The overall accuracy, sensitivity and specificity value achieved are 87.0%, 96.4% and 0% for optic disk in ROP Infant. In infant's retinal image, the overall specificity result is 0 because the algorithm does not detect the pixels which non-optic disk pixels which were correctly identified as non-optic disk pixels. For all other retinal images, the accuracy results were detected by the proposed method is acceptable. However, all of thirty optic disks from low-contrast images were identified by this proposed algorithm.

V. CONCLUSION AND DISCUSSION

We have presented a method for Optic Disk detection based on Mathematical Morphology. The blood vessel was removed by using morphological closing. The shape of optic disk was extracted by using dilation, erosion and connected component. The results were validated against clinicians' hand-drawn ground truth. The result optic disk ROP Infant is quite successful with accuracy of 87.8%. This method is able to identify correct position of all optic disk in ROP Infant. One visible advantage of this algorithm, it works pretty well on low-contrast retinal image in ROP Infant, fast computation and reliable. Finally, this algorithm will help the clinicians to analyze the area surrounding the optic nerve which is predictive of the level of ROP.

ACKNOWLEDGEMENT

We would like to thank Kington University, UK and Thammasat university hospital, Thailand who supplied all the images used in this paper.

REFERENCES

[1] M. Foracchia, E. Grisan, and Ruggeri. "Detection of Optic Disc in Retinal Images by Means of a Geometrical Model of Vessel Structure," IEEE Transactions on Medical Imaging, Vol. 23, NO. 10, 2004.

[2] K. Akita and H. Kuga, "A computer method of understanding ocular fundus images," Pattern Recognition., vol. 15, pp. 431-443, 1982

[3] M. Lalonde, M. Beaulieu, and L. Gagnon. "Fast and robust optic disk detection using pyramidal decomposition and Hausdorff-based template matching," IEEE Transactions on Medical Imaging, Vol. 20, No. 11, 2001.

[4] H. J. Kong, S.K. Kim, J.M. Seo, K. H. Park, H. Chung, K.S. Park, and H.C. Kim. "Three Dimensional Reconstruction of conventional Stereo Optic Disc Image, " Annual International Conference of the IEEE EMBS, Sep. 2004.

[5] M.J. Cox, I.C.J. Wood. "Computer-Assisted Optic Nerve Head Assessment." Ophthal. Physiol. Opt. Vol. 11 1991, pp 27-35.

[6] D.T. Moris, M.J. Cox, I.C.J. Wood. "Automated Extraction of The Optic Nerve Head Rim." American Association of Optometrists Annual Conference, Boston,Dec. 1993.

[7] C. Sinthanayothin, J.F. Boyce, H.L. Cook, and T.H. Williamson, "Automated localization of the optic disc, fovea, and retinal blood vessels from digital color fundus images," Br J. Ophthalmol., vol. 83, pp. 902-910, Aug. 1999.

[8] S. Lee, "Visual Monitoring of Glaucoma", Ph.d., Robotics Research Group Department of Engineering Sceince, University of Oxford, 1991, Available on micro-fiche.

[9] H. Li, and O. Chutatape "Automatic Location of optic disk in retinal images" 2001 IEEE

[10] H. Li and O. Chutatape, "Boundary detection of optic disk by a modified ASM method". Pattern Recognition. v36 i9. 2093-2104.

[11] D. Kavitha, S. Shenbaga Devi, , "Automatic Detection of Optic Disc and Exudates in Retinal Images", IEEE Int. Conf. On Intelligent Sensing and Information Processing (ICISIP), pp. 501-506, Jan 2005.

[12] Jelinek, H.F., Depardieu, C., Lucas, C. Cornforth, D., Huang, W. And Cree, M.J., 2005, Towards vessel characterisation in the vicinity of the optic disk in digital retinal images. McCane (ed.), *Proceedings of the Image and Vision Computing Conference*, New Zealand 2005, University of Otago.

[13] A.Osareh, M. Mirmehdi, B. Thomas, and R.Markham. "Colour Morphology and Snakes for Optic Disc Localisation," The 6th Medical Image Understanding and Analysis Conference, Jul. 2002.

[14] F. Mendels, C. Heneghan, J.P. Thiran, "Identification of the optic disc boundary in retinal images using active contours", in: Proceedings of the IMVIP Conference, 1999, pp. 103-115.

[15] T. Chanwimaluang and G. Fan, "An efficient algorithm for extraction of anatomical structures in retinal images," in *Proc. IEEE International Conference on Image Processing*, pp. 1093–1096, (Barcelona, Spain), 9 2003.

[16] R.C. Gonzalez, R.E.Woods, "Digital Image Processing 2nd Edition", Prentice Hall, New Jersey, 2002, ISBN: 0-201-18075-8.

[17] L. Costaridou. Medical Image Analysis Methods. CRC Press, New York, 2005, pp. 438-440.